



Simulation Analysis of Pseudo-dynamic Test of Resilient Prefabricated Prestressed Steel Frame

Yanxia. Zhang⁽¹⁾, Anran. Liu⁽²⁾, Xuechun. Liu⁽³⁾, Hexin. Zhang⁽⁴⁾, Hui. Wu⁽⁵⁾

⁽¹⁾ Associate Professor, School of Civil and Transportation Engineering, Beijing University of Civil Engineering and Architecture, zhangyanxia@bucea.edu.cn

⁽²⁾ Master Candidate, School of Civil and Transportation Engineering, Beijing University of Civil Engineering and Architecture, appleanran@163.com

⁽³⁾ Associate Professor, College of Architecture and Civil Engineering, Beijing University of Technology, liuxuechun@bjut.edu.cn

⁽⁴⁾ Master Candidate, School of Civil and Transportation Engineering, Beijing University of Civil Engineering and Architecture, 124255576@qq.com

⁽⁵⁾ Professor, School of Civil and Transportation Engineering, Beijing University of Civil Engineering and Architecture, wuhui@bucea.edu.cn

Abstract

Resilient prestressed steel frame (RPSF) can reduce structural damage, reduce or eliminate residual deformations, and are easy to repair after a strong earthquake. However, this type of structural system requires on-site aerial tension in high-rise buildings. Therefore, the new structure system resilient prefabricated prestressed steel frame (RPPSF) for high-rise buildings and performance-based design method were put forward by authors, which avoids the potential issues of aerial PT operations. The beam of the resilient prefabricated prestressed steel frame (RPPSF) is divided into three parts: a long-beam portion and two short-beam portions at both ends. These parts are connected with a vertical plate, and PT high-strength strands run parallel to the beam. Brass plates are sandwiched between the webs of the beam and the friction plates so as to achieve reliable friction performance and dissipate energy. The entire assembly is connected to the column similar to a traditional beam. A four-story 3×5 span prototype structure was design and the 0.75 scale substructure pseudo-dynamic test was conducted.

In this thesis, a finite element model using software ABAQUS aims at investigating the dynamic mechanical behavior of resilient prefabricated prestressed steel frame (RPPSF) and simulating the process of pseudo-dynamic test has been established. Through comparing the results of finite element analysis (FEA) and the pseudo-dynamic test, RPPSF is proved to have a good gap opening and closing mechanism, favorable energy dissipating capacity, structural self-centering and recovering function after the rare seismic actions. Additionally, numerical results are in coincidence with that from the test basically, revealing the fact that the finite element method is capable enough of simulating the actual state of the pseudo-dynamic test, and is reliable in the predicting compensating the real structure responses results respectively. Moreover, FEA provides visual results for the plastic strain developing variation of the structural members, presenting the plasticity development process with the intensification of the seismic actions more visually, and having research on the strain condition the test cannot reach. Last but not the least, for the FEA model has the characteristics to be able to apply more ideal boundary conditions and loads on the structure, resolve the problems that cannot be solved in real test such as resolving the problem that unsymmetric stiffness appeared at both ends, it may both enable a thorough dynamic mechanical behavior analysis towards the new structure system RPPSF and lay the foundation for the space test of it.

Keywords: Resilient Prestressed Steel Frame; Resilient Prefabricated Prestressed Steel Frame; Friction Damper; Pseudo-dynamic Test; Finite Element Analysis.

1. Introduction

Resilient prestressed steel frame (RPSF) can reduce structural damage, reduce or eliminate residual deformations, and are easy to repair after a strong earthquake. In the last decade, a large number of experimental and theoretical studies focusing on self-centering post-tensioned steel frame [1,2,3,4,5] accompany with the researching development of steel connections with self-centering functions [6,7,8,9] have been carried out, verified that the RPSF have a favorable aseismic performance and recovering functions. However, this type of structural system requires on-site aerial tension in high-rise buildings. The new resilient prefabricated prestressed steel frame (RPPSF) with web friction damper for high-rise buildings and performance-based design method were put forward by authors, which avoids the potential issues of aerial PT operations. Additional experiment on the connections, theoretical analysis and numerical simulation have been carried out [10]; A four-story 3×5 span prototype structure was design and the 0.75 scale substructure pseudo dynamic test was conducted [11]. In order to achieve the deformation and stress distribution results of the critical joint and the control section under the seismic action with the consideration of the dynamic effect of the structure, the solid elements would be utilized to establish the finite element model and therefore, to carry out the numerical simulation and the analysis toward the structure response to the seismic actions, investigating and the dynamic mechanical performance of RPPSF. Additionally, the analysis results achieving from FEA would compare with those from the completed pseudo-dynamic test to verify the reliability of the FEA method and provide a solution and evidence to the results prediction of substructure in pseudo-dynamic test in the further research.

2. Details of the RPPSF

The RPPSF consists of frame columns, self-centering beam and ordinary frame which are illustrated in detail in Fig.1. Self-centering beam of the RPPSF consists of three parts: a long-beam portion and two short-beam portions at both ends and three parts are connected with a vertical plate at each ends of the short beam, and post-tensioned high strength strands run parallel to the beam. Brass plates are sandwiched between the webs of the beam and the friction plates to achieve reliable friction and dissipate energy. The entire assembly is connected to the column similar to a traditional beam. Columns in RPPSF are designed to be rigid at the column bases, which other details of them are same as the moment resistant frame. Additionally, the joint panel should under the control of *Strong Column and Weak Beam* principle specified in Chinese *Code for Seismic Design of Buildings* [12], i.e., the failure of the column should be avoided before the beam has reached the ultimate limited state. Therefore, RPPSF advances in avoiding potential issue of the on-site aerial PT operations for high-rise buildings and the perforations on the column flanges for steel strands setting use, decreasing the construction difficulties under the premise of ensuring the construction quality and shortening the construction time.

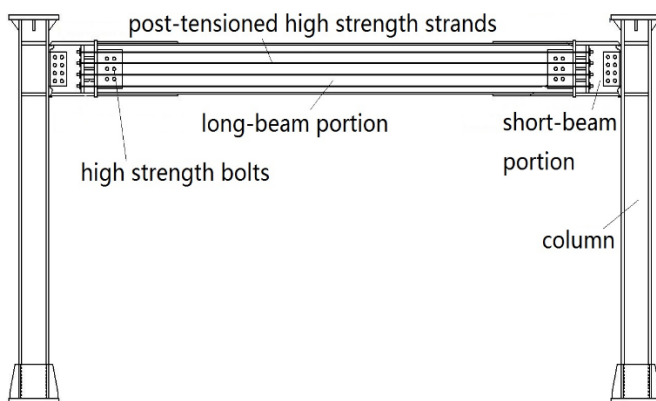


Fig. (a) Tested frame

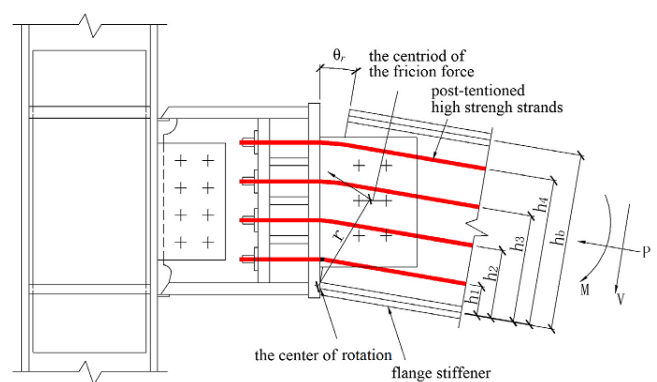


Fig. (b) Schematic figure of PSC connection gap opening

Fig.1 Resilient Prefabricated Prestressed Steel Frame

3. General condition of RPPSF pseudo-dynamic test

The structural plan of RPPSF prototype is shown in Fig.2. There are 3×5-bays, where all spans were 8m. The height of the first floor was 3.9m, and the height of floors 2 to 4 were 3.6m. The high-light area represents the frame beams and columns adapted post-tensioned self-centering beam–column connections; that the frame columns are in box section of $\square 400 \times 400 \times 34$, and the frame beams are H-section beam of $H588 \times 200 \times 12 \times 20$. The other parts are hinge systems, which had $\square 400 \times 400 \times 34$ columns and $H588 \times 200 \times 12 \times 20$ beams. Pseudo-dynamic tests were conducted on the 1-story 0.75 scale experimental sub-structure of RPPSF with web friction devices, where the height of the first floor was 3.15m, and the height of floor 2-4 were 2.7m, the frame columns were in H section of $H300 \times 300 \times 20 \times 30$, the long-beam portions were in $H450 \times 250 \times 14 \times 16$, and the short-beam portions were $H450 \times 250 \times 14 \times 30$, 10.9 grade M20 energy dissipating bolts were adapted in post-tensioned self-centering beam–column connections and beam-column connections either. The post-tensioned strands were the 1×19 type with a nominal tensile strength of 1860MPa, and the value of the initial force was 25% of the tensile limit (0.25Tu). The 2-4 story of the structure is the numerical operated substructure which is shown in Fig.3

LOS000, EL-Centro and Taft ground motions are selected during the pseudo-dynamic test, which the peak values of the seismic acceleration record (PGA) are 0.07g, 0.2g, 0.4g and 0.51g corresponding to the specifications for the 8-degree frequent, design, rare and 8.5-degree rare seismic actions respectively in accordance with Chinese *Code for Seismic Design of Buildings* [12]. As the pseudo-dynamic test photograph illustrating in Fig.4, the structure displacement, the gap-opening variation of beam-column joint, the bearing capacity of the structure, the energy dissipating capacity and the strain variation have been achieved under different ground motions with various seismic actions. The test results indicate that the structure remains in the state without the plasticity development and structural damage under seismic action of $PGA=0.07g$ and $PGA=0.2g$. Moreover, excepting the reinforced plate of the long beam portions, the strain has not exceed twice of the yielding strain in the web of the panel zone, the flange of the panel zone, the flange and the web of the column base and the flange of the short beam portions, indicating that the main structure can still have favorable serviceability, and the target of recovering the structure function can be realized after undergoing the various seismic actions.

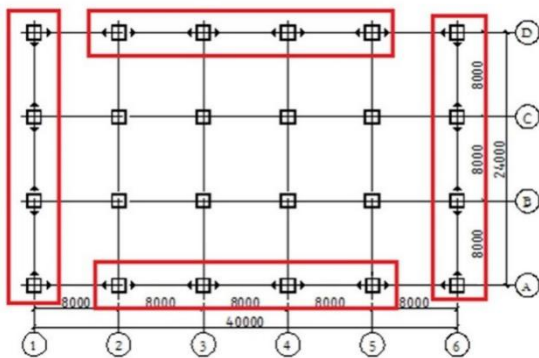


Fig.2 Plan schematic of prototype structure

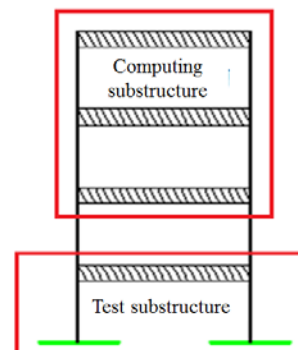


Fig.3 Schematic of the substructures



Fig.4 Test photograph

4. Finite element analysis (FEA)

4.1 Construction of a finite element model

4.1.1 Unit selection and mesh generation

The member sizes of the RPPSF established for the FEA are scaled down to 0.75 compared with the prototype structure which are same as the experimental dimensions. The main body of the RPPSF finite element model adapts C3D8R solid element, and post-tensioned strand adapts T3D3 truss unit. Having given consideration to both calculation accuracy and computational efficiency, approximate global size of grid seeds of main body of the beams and columns is 200mm, joints and the reinforced part of the beam flange is 60mm, to where the friction interactions have been defined such as beam webs and junction plates is 30mm. The mesh generation of the RPPSF model is shown in Fig. 5.

4.1.2 Unit selection and mesh generation

The impact of geometric and material nonlinearities was considered in the model calculation. The steel material used for the test specimens was Q345B which adapted Von Mises criterion and kinematic hardening criterion. The elastic property of the steel was defined by the elastic modulus (E) and Poisson ratio (ν), while the plastic property data were given in the form of the stress-strain curve. According to the material test data, $E=2 \times 10^5 \text{MPa}$ and $\nu=0.3$ were used. The PT strand was in the elastic state, and thus, only the elastic modulus and Poisson ratio were defined.



Fig. 5 The mesh generation of the ICSCSF model

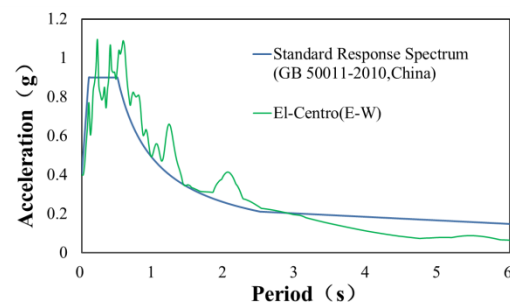


Fig. 6 Acceleration response spectrum



4.1.3 Boundary and load conditions

The boundary and load conditions were same with the test. In the finite element model, six degrees of freedom at the bottom of the columns were all fixed. Acceleration time history was exerted upon the RPPSF finite element model directly, aiming at investigating the seismic behavior of the RPPSF. Acceleration response spectra of the El-Centro (E-W) earthquake ground motion shown in Fig.6 were used in the finite element numerical simulation that was same as one of earthquake ground motions selected in the pseudo-dynamic test; that the various peak values of seismic actions input in the FEA were same as the test either. The time step for the EL-Centro (E-W) data was scaled to 0.0086s.

4.1.4 Algorithm selection

The FEA is carrying out in the Abaqus/Standard module, with the adaption of the implicit dynamic step accomplishing the calculation. The algorithm used to proceed the implicit nonlinear dynamic analysis in software Abaqus6.11 includes Transient fidelity applications, Moderate dissipation applications and Quasi-static applications, which the Quasi-static applications adapt the Backward Euler method to solve the dynamic equations, analyzing the dynamic problems by dividing them into static problems. During the calculation with the application of Quasi-static method, the inertial force of the structure can be achieved by solving the dynamic equations and then can be implemented on the structure in way of quasi-static method, which the dynamic impact effect is reduced to a very significant extent. Therefore, Quasi-static applications are adapted to simulate the pseudo-dynamic test.

4.2 Comparison to RPPSF FEA and test results

Structure responses results are selected according to the first 15 seconds of the structural displacement time history, and data processing methods to both kinds of results are in the same in reference to *Pseudo dynamic test study of resilient prefabricated prestressed steel frame* [11].

4.2.1 Displacement response

Fig.7 shows the comparison of displacement response of the FEA and the pseudo-dynamic test results under seismic action of EL-Centro ground motion of PGA=0.07g, 0.2g, 0.4g and 0.51g. The time-history curve of the displacement response achieved from the FEA and the testing results are in coincidence comparatively, especially the displacement time-history curves are in very coincidence in the first 6-8 seconds of the whole duration of the seismic actions.

Table 1 lists the maximum displacement responses and the interstory drifts on two sides of the structure. Under the seismic action of PGA=0.07g, the maximum displacement to the east of the plane frame from test and FEA is 17.21mm and 14.30mm respectively, with corresponding interstory drift is 1/218 and 1/222 respectively; that under the seismic action of PGA=0.2g, the maximum displacement for same position increases to 30.65mm and 35.62mm respectively, with corresponding maximum displacement to the west of the plane is 41.08mm and 34.65mm respectively. Maximum displacement on two sides of the plane frame from FEA is in less than the difference compared with the results achieved from the test, which indicating a favorable predictability to the results of test structure in advance and a potent supplement to the analysis of the structure afterwards.

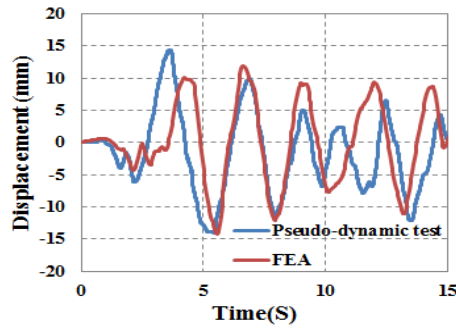


Fig.7 (a) 0.07g

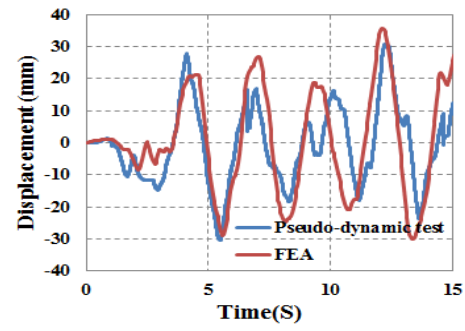


Fig.7 (b) 0.2g

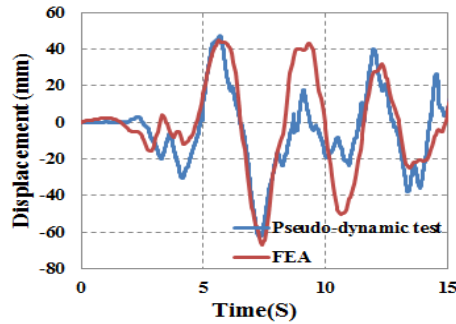


Fig.7 (c) 0.4g

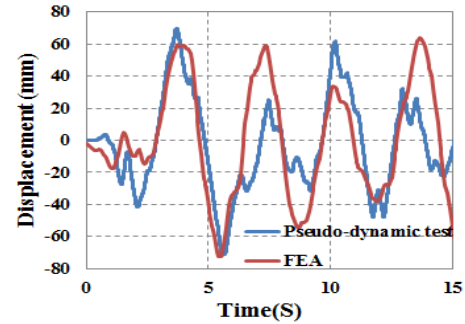


Fig.7 (d) 0.51g

Fig.7 Displacement time-history curve

As can be seen from Table 1, under the seismic action of PGA=0.4g, the maximum displacement to the east of the plane frame from test and FEA is 62.20mm and 66.88mm respectively, with corresponding interstory drift valued 1/50 and 1/47 respectively, and the maximum displacement to the west of the plane from both results is 81.37mm and 60.13mm with the corresponding interstory drift valued 1/39 and 1/52 respectively. The different displacement response on two sides of the plane frame from the test is more apparent with the increase of the seismic actions, the maximum displacement on two sides of the plane frame from FEA is still in less than the difference though difference increases compared with that under seismic action of PGA=0.4g. Under the seismic action of PGA=0.51g, structure response of experimental structure peaks, the maximum displacement to the east of the plane frame from test and FEA is 71.53mm and 72.57mm respectively, with corresponding interstory drift valued 1/44 and 1/43 respectively, and the maximum displacement to the west of the plane from both results is 91.80mm and 82.41mm with the corresponding interstory drift valued 1/34 and 1/38 respectively, exceeding the elastic-plastic interstory drift limit of the steel frame specified in standards GB 50011-2010, 2010, indicating the reliability of predicting the test results through FEA.

Table 1 Comparison of the major results under 8-degree frequent seismic actions

EL-Centro		Maximum base shear (kN)	Maximum displacement(mm)		Maximum interstory drift (rad)	
			East	West	East	West
PGA=0.07g	Test	244.02	17.21	19.39	1/218	1/162
	FEA	209.40	14.30	15.39	1/222	1/204
PGA=0.2g	Test	571.52	30.65	41.08	1/103	1/77
	FEA	641.67	35.62	34.65	1/88	1/92
PGA=0.4g	Test	914.51	62.2	81.37	1/50	1/39
	FEA	964.93	66.88	60.13	1/47	1/52
PGA=0.51g	Test	1072.22	71.53	91.80	1/44	1/34



FEA	1107.15	72.57	82.41	1/43	1/38
-----	---------	-------	-------	------	------

4.2.2 Gap openings

Under the seismic action of the EL-Centro ground motion of $PGA=0.07g$, there is no generation of the gap-opening at the joints. The joints gap openings were formed under the seismic action of $PGA=0.2g$. Table 2 lists the comparison of the FEA results and pseudo-dynamic test results about gap opening rotation and residual rotation of the joints on the east and west side. In the maximum gap-opening of the joint respect, the result of FEA is in very coincidence with that of test. The maximum gap-opening appears under the seismic action of $PGA=0.51g$, which the gap-opening conditions on the western side of the structure is illustrated in Fig.9; the maximum gap opening is 2.54%rad and 3.23%rad on two sides of the experimental plane structure respectively, while the maximum gap opening achieved from FEA is 3.05%rad and 3.18%rad on two sides respectively, which still indicates a favorable symmetric behavior, though the lateral displacement and the gap opening differences of both sides from FEA increases evidently for large deformations.

The maximum residual rotation is an important index in evaluating resilient capacity. The structure can be in an elastic state basically without residual rotation while under seismic action of $PGA=0.07g$. As gap opening generating at the interface of long beam and short beam portions with activating aseismic mechanism through self-centering function, the resilient capacity of the structure can be reflected by the value of the residual rotation. Table 2 shows that the maximum residual rotation is little either in FEA or in test, which the FEA value only reaches 0.06%rad on west side under seismic action of $PGA=0.2g$. Under the seismic action of $PGA=0.51g$, the maximum residual rotation to the east and west of the plane frame from test is 0.24% and 0.07% respectively, and the results from FEA is 0.23% and 0.22%, respectively. The residual rotation of the structure remains minor, therefore, although the considerable maximum displacement of the structure exceeds the elastic-plastic interstory drift limit of the steel frame specified in standards under $PGA=0.51g$, the structure can still recover to the initial position, indicating a favorable resilient capacity.

Table 2 Comparison of the major results under 8-degree frequent seismic actions

EL-Centro		Maximum gap-opening rotation (%rad)		Maximum residual rotation (%rad)	
		East	West	East	West
PGA=0.07g	Test	—	—	—	—
	FEA	0.09	0.08	—	—
PGA=0.2g	Test	0.63	0.89	0.02	0.03
	FEA	1.17	1.17	0.03	0.06
PGA=0.4g	Test	1.92	2.78	0.04	0.09
	FEA	2.29	2.26	0.11	0.11
PGA=0.51g	Test	2.54	3.23	0.24	0.07
	FEA	3.05	3.18	0.23	0.22



Fig.8 (a) The opening on western side is 14.04mm, the gap-opening is 2.23%

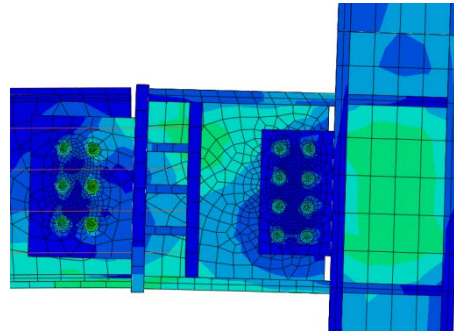


Fig.8 (b) The opening on western side is 13.80mm, the gap-opening is 3.18%

Fig.8 Plane frame gap-opening comparison between FEA and test (PGA=0.51g)

4.2.3 Hysteretic behavior

The base shear-displacement curve of the model structure presented in Fig.9. Under the seismic action of the EL-Centro ground motion of PGA=0.07g, the hysteresis loop of the structure is linear, indicating apparent elastic characteristic and favorable initial rigidity coincidence, for there is no generation of the gap-opening at the joints. Hysteretic loops of the structure from both the test and FEA results begin appearing because of the beam-column connections opening and the friction dampers dissipating energy under the seismic action of PGA=0.2g. Under the seismic action of PGA=0.4g, the maximum displacement and the base shear of both structures are in coincidence basically in both negative and positive direction, the maximum base shear from test and FEA is 964.93kN and 914.51kN, respectively. The hysteresis loops of the structure from both the test and FEA results plump significantly for the energy dissipated by the web friction dampers accompany with the increasing gap-opening under the intensifying seismic actions. After the gap opening happens, hysteretic curves bends evidently, indicating the stiffness reduction of the structure with the appearance of the structure. Therefore, the FEA simulates the actual state of the structure regarding the stiffness variation before and after the appearance of gap opening. Under the seismic action of PGA=0.51g, the maximum base shear from test and FEA is 1072.22kN and 1107.15kN, respectively, the maximum displacement and the base shear of both structures are still in coincidence basically in both negative and positive direction. As gap opening continued developing, the stiffness variation of the structure before and after the appearance of gap opening can be reflected through the hysteretic curves. The hysteresis loops of the structure from both the test and FEA results plump sequentially for the energy continued dissipated by the web friction dampers, demonstrating the double-flag shaped hysteretic model as the result, indicating the outstanding resilient performance of RPPSF.

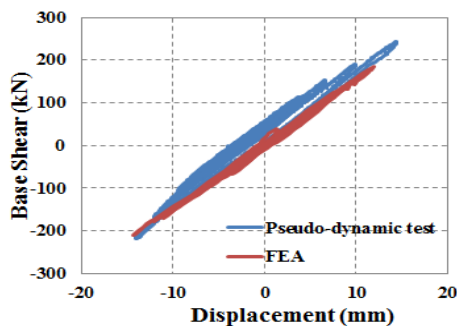


Fig.9 (a) 0.07g

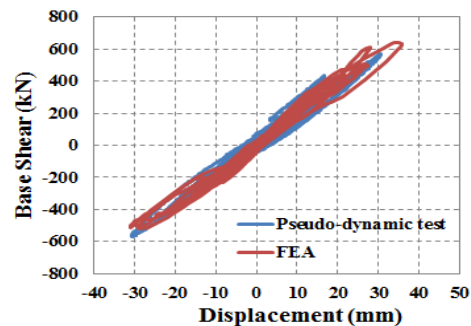


Fig.9 (b) 0.2g

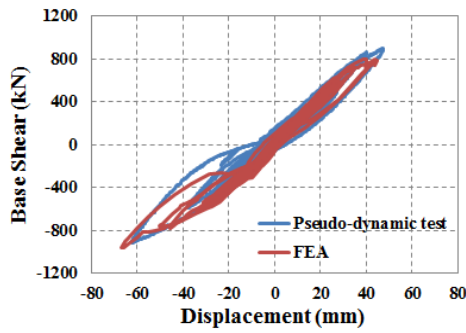


Fig.9 (c) 0.4g

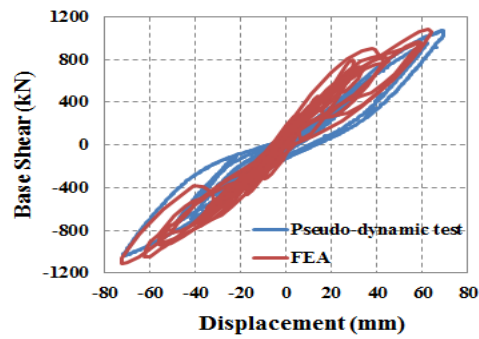


Fig.9 (d) 0.51g

Fig.9 Base shear force-displacement response from EL-Centro

4.2.4 Strain condition

To the variation of the strain, the structure remains elastic under $PGA=0.07g$ and be in an elastic state basically under $PGA=0.2g$ both in the FEA and test results. Under the seismic action of $PGA=0.4g$, the strain data to where the plasticity develops during the test is shown in Table 3, while the diagrams of equivalent plastic strain are given in Fig.10. The plasticity firstly develops at the reinforced plate to the east upper flange of the beam, then appears at the center of the upper flanges closer to the western short portion beams, the western panel zone and tensile side of the western column base flanges successively. The maximum residual rotation is an important index in evaluating resilient capacity. The structure can be in an elastic state basically without residual rotation while under seismic action of $PGA=0.07g$. As gap opening generating at the interface of long beam and short beam portions with activating aseismic mechanism through self-centering function, the resilient capacity of the structure can be reflected by the value of the residual rotation. Table 2 shows that the maximum residual rotation is little either in FEA or in test, which the FEA value only reaches 0.06% rad on west side under seismic action of $PGA=0.2g$. Under the seismic action of $PGA=0.51g$, the maximum residual rotation to the east and west of the plane frame from test is 0.24% and 0.07% respectively, and the results from FEA is 0.23% and 0.22% , respectively. The residual rotation of the structure remains minor, therefore, although the considerable maximum displacement of the structure exceeds the elastic-plastic interstory drift limit of the steel frame specified in standards under $PGA=0.51g$, the structure can still recover to the initial position, indicating a favorable resilient capacity.

Table 3 Maximum strain of elements section under $PGA=0.4g$ in test ($\mu\epsilon$)

EL-Centro	Short portion beam flanges	Long beam portions flanges	Reinforced plate	Web of the panel zone	Flange of the column base	Web of the column base
0.4g	3296	1265	4734	1806	2951	2240

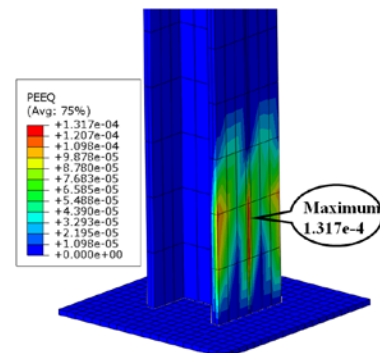
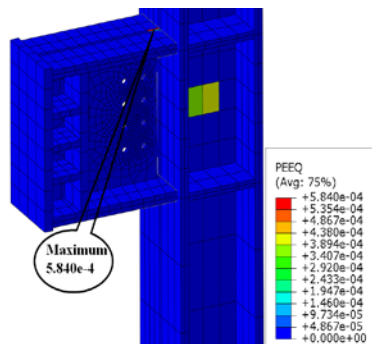
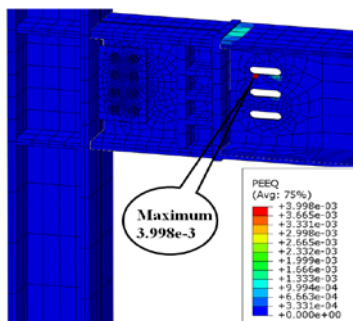




Fig.10 (a) The plastic developing condition of reinforced plate

Fig.10 (b) The plastic developing condition of the panel zone

Fig.10 (c) The plastic developing condition of column base

Fig. 10 PEEQ diagram of elements under PGA=0.4g

The stain variation of the test under PGA=0.51g is shown as Table 4. As the finite element analysis results shown in Fig. 11, plasticity develops at the eastern panel zone, the tensile side of the eastern column base flanges, the web of the short beam portions and both sides of the column base flanges successively with the plasticity expanding in the plastic area concluded under PGA=0.4g. The maximum equivalent plastic strain has transited to the western column base flanges valuing $8.016e-3$, indicating that the column base flanges and partial of the interface region of web and flanges have yielded, while the plastic area has not grown through the web and realized the formation of the plastic hinge, verifying that the column base still have the flexural capacity that shall be regarded as the rigid connections. The equivalent plastic strain at center of the upper flanges closer to the eastern short portion beams is $7.766e-3$ which values secondly, then are the reinforced plates ends of the long beam portion flanges and the panel zones, which the equivalent plastic strain varies from $1e-3$ to $4e-3$ with the ends of the reinforced plates coming into yield states. The panel zone on both sides of the beam yields with the maximum equivalent plastic strain $1.893e-3$ appearing at the central area of the panel zone, as well as the plasticity developing area approaching the whole panel zone. Through the FEA, it can be ascertained that the plasticity generates at webs of short beam portions on both sides with the maximum equivalent plastic strain valuing $4.469e-4$. Due to the complicated stress state resulting from combined action of moment, shear force and tension of the steel strands, the webs of short beam portions on both sides have very possibility to be in the yielding states. The results concluded above could not be achieved through the test due to the space limitation, which can be compensated by the utilization of the finite element analysis.

The test results indicate that, under PGA=0.51g, the maximum plastic strain appears at the reinforced plates. The maximum plasticity transits from the reinforced plates to the column base flanges in the finite element analysis results for the rigid connecting effect is more ideal in the numerical simulation, predicting that it is very significant to resolve plasticity development at the column bases in RPPSF.

Table 4 Maximum strain of elements section under PGA=0.51g in test ($\mu\epsilon$)

EL-Centro	Short portion beam flanges	Long beam portion flanges	Reinforced plate	Web of the panel zone	Flange of the column base	Web of the column base
0.51g	4507	1394	7273	3094	3167	2663

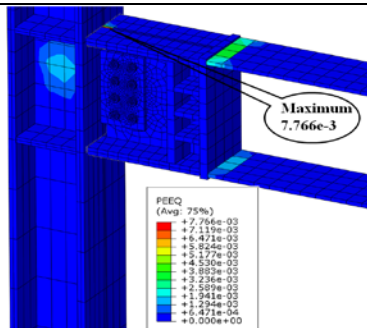


Fig.11 (a) The plastic developing condition of reinforced plate

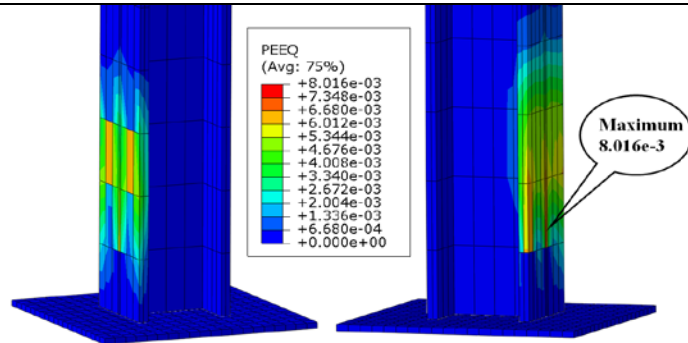


Fig.11 (b) The plastic developing condition of column base

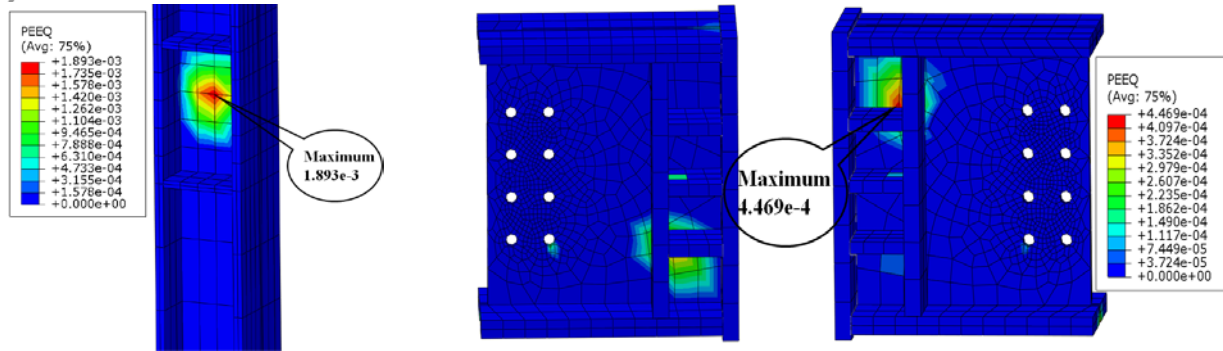


Fig.11 (c) The plastic developing condition of panel zone

Fig.11 (d) The plastic developing condition of short portion beam

Fig. 11 PEEQ diagram of elements from EL-Centro under PGA=0.51g

5. Conclusions

(1) With the utilization of the finite element method, the numerical simulation towards the pseudo-dynamic test of RPPSF was carried out. The data and results concerning the displacement response, the variation of gap-openings, the hysteretic loops reflecting the variation of structural stiffness and the plastic strain development achieved from FEA, where the FEA software ABAQUS was adopted, were in coincidence with those obtained from the pseudo-dynamic tests basically; verified that the finite element analysis is reliable and capable to simulate the actual state of the pseudo-dynamic tests to a large extent, as well as to predict the structural responses respectively.

(2) FEA provides visual results for the plastic strain developing variation of the structural members, presenting the plasticity development process with the intensification of the seismic actions more visually, and having research on the strain condition the test cannot reach. The plasticity firstly developed at the reinforced plate to the east upper flange of the beam under the seismic actions of PGA=0.4g, and with the intensification of the seismic actions, it extended to the short beam flanges, joint panels and the column bases successively accompanied with the plastic area expansion, and the developed at local region of short beam webs in the end under the seismic actions of PGA=0.51g.

(3) For the FEA model has the characteristics to be able to apply more ideal boundary conditions and loads on the structure, resolve the problem that unsymmetric stiffness appeared at both ends during in the test, it may both enable a thorough dynamic mechanical behavior analysis towards the new structure system RPPSF and lay the foundation for the space test of it. FEA resolved the problems appeared in the pseudo-dynamic test, that the asymmetric stiffness occurred on two sides of RPPSF due to the application of the loading end that to satisfy the loading requirement. Additionally, RPPSF was subjected to inertial force action more evenly by exerting the time-history acceleration upon the finite element model directly; there the seismic action could be simulated more favorably. As a conclusion, the FEA have the ability to compensate for the results achieved from the pseudo-dynamic test, as well as to predict and simulate the actual structural responses under the real seismic actions.

6. Acknowledgements

The research reported herein is supported by the National Natural Science Foundation of China under Grant No. 51278027 and the Key Project of Beijing Natural Science Foundation under Grant No.8131002.



7. References

- [1] Garlock M, Ricles J M, Sause R (2008): Influence of design parameters on seismic response of post-tensioned steel MRF systems. *Journal of Engineering Structures*, **30**,1037-1047.
- [2] Rojas P, Ricles. J M, Sause R (2005): Seismic performance of post-tensioned steel moment resisting frames with friction devices. *Journal of Structural Engineering*, **131**(4), 529-540.
- [3] Kim H, Christopoulos C (2008): Friction damped post-tensioned self-centering steel moment-resisting frames. *Journal of Structural Engineering*, **134**(11), 1768-1779.
- [4] Iyama J, Seo C Y, Ricles J M, Sause R (2009): Self-centering MRFs with bottom flange friction devices under earthquake loading. *Journal of Constructional Steel Research*, **65**, 314-325.
- [5] Lin Y C, Sause R, Ricles J (2013): Seismic performance of a large-scale steel self-centering moment-resisting frame: MCE hybrid simulations and quasi-static pushover tests. *Journal of Structural Engineering*, **139**(7), 1227-1236.
- [6] Ricles J, Sause R, Garlock M, Zhao C (2001): Post-tensioned seismic-resistant connections for steel frames. *Journal of Structural Engineering*, **127** (2), 113-121.
- [7] Christopoulos C, Filiatrault A, Uang C M, Folzb (2002): Post-tensioned energy dissipating connections for moment-resisting steel frames. *Journal of Structural Engineering*, **128**(9), 1111-1120.
- [8] Rojas P, Ricles. J M, Sause R (2005): Seismic performance of post-tensioned steel moment resisting frames with friction devices. *Journal of Structural Engineering*, **131**(4), 529-540.
- [9] Wolski M, Ricles M, Sause R (2009): Experimental study of a self-centering beam-column connection with bottom flange friction device. *Journal of Structural Engineering*, **135**(5), 479-488.
- [10] Zhang A.L.,Zhang Y.X., Li R, Wang Z.Y. (2016): Cyclic behavior of a prefabricated self-centering beam-column connection with a bolted web friction device. *Engineering Structure*, **111**, 185-198.
- [11] Zhang A.L.,Zhang Y.X., Zhao W and Fei C.C. (2016): Pseudo dynamic test study of resilient prefabricated prestressed steel frame.*Journal of Vibration and Shock*, **35**(5),207-215
- [12]GB 50011-2010 (2010):*Code for seismic design of buildings*. Beijing:China Architecture & Building Press.(in Chinese).